

MELTING/FREEZING IN NARROW PORES; DIELECTRIC AND EPR STUDIES

M. ŚLIWIŃSKA-BARTKOWIAK¹, G. DUDZIAK¹, M. KEMPIŃSKI¹,
W. KEMPIŃSKI², R. RADHAKRISHNAN³, F. HUNG⁴, K. E. GUBBINS⁴

¹*Institute of Physics, Adam Mickiewicz University
Umultowska 85, 61-614 Poznań, Poland*

²*Institute of Molecular Physics, Polish Academy of Sciences
M. Smoluchowskiego 17, 60-179 Poznań, Poland*

³*Courant Institute of Mathematical Sciences, New York University, 31
Washington Place, New York, NY 10003, U.S.A.*

⁴*Department of Chemical Engineering, North Carolina State University,
Raleigh, NC 27695-7905, U.S.A.*

Abstract. We report results of a study of the phenomena associated with melting of nano-phases confined within narrow pores. The study was performed by differential scanning calorimetry, dielectric spectroscopy, nonlinear dielectric effect measurements and electron paramagnetic resonance. Results of theoretical calculations concerning the phenomena are also presented. It has been proved, by experimental and theoretical methods, that the phenomena of melting in nano-phases are accompanied by the appearance of new phases (contact layer phases, hexatic phase), the nature of which depends on the structure of the walls and the pore size. The melting temperatures also depend strongly on these factors.

1. Introduction

The aim of this paper is to present phenomena associated with freezing and melting of nano-phases confined within narrow pores, using calorimetric, dielectric and spectroscopic (EPR) methods. Questions of interest in this field include the following: Is there a first order phase transition? What is the effect of confinement on the freezing temperature and how does this vary with the pore size, pore shape, the nature of the material and confined substance? What new phases, if any, occur that are not observed in bulk systems? What is the effect on the enthalpy change on transition? These questions are of fundamental scientific interest. In addition, an understanding of freezing in confined systems is of practical importance in lubrication, adhesion, and nanotribology. Freezing in narrow pores is important in understanding frost heaving and the distribution of pollutants in soils. Freezing in porous media has also been widely employed in the characterization of porous materials using the method of thermoporometry [1]. In this method the change in the freezing temperature is related to the pore size through the Gibbs-Thomson equation.

Prior to our work, relatively few experimental studies had been carried out, primarily for freezing of fluids in silica-based materials with pores of roughly cylindrical geometry. These experiments showed a lowering of the freezing temperature relative to the bulk value, $\Delta T_f = (T_{f,pore} - T_{f,bulk}) < 0$. For a porous medium with sufficiently large pores, the Gibbs-Thomson equation (the freezing analogue of the Kelvin equation for condensation), relates the shift in the freezing temperature to the surface tensions (γ) involved and pore width (H) by the equation:

$$\frac{\Delta T_f}{T_{f,bulk}} = -2 \frac{(\gamma_{ws} - \gamma_{wl})v}{H\lambda_{f,bulk}} \quad (1)$$

where subscripts w , s and l indicate wall, (confined) solid and (confined) liquid, respectively, and v and λ_f are the molar volume and latent heat of fusion for the bulk liquid. This equation, which predicts a linear relation between the shift in freezing temperature and H^{-1} , is based on classical thermodynamic arguments, and neglects effects due to the inhomogeneity of the confined phase and to intermolecular interactions with the wall. It will break down for small pores.

2. Experimental Studies

The experimental methods used were: differential scanning calorimetry (DSC), dielectric relaxation spectroscopy (DRS), nonlinear dielectric effect (NDE) measurements and electron paramagnetic resonance (EPR). In DSC phase transitions appear as sharp peaks at the transition temperature, and the area under the peak gives the enthalpy release (or adsorption) for the transition. DSC is a relatively simple and quick measurement to perform. However, it does not give information about the nature of the phases involved beyond the latent heat of transition, and subtle transitions, such as contact layer phases are difficult to detect. In DRS the complex relative permittivity of the system, $\kappa^* = \kappa' - i\kappa''$, is measured by applying an alternating electrical potential to the system, whose frequency can be varied over a wide range. Here κ' is the dielectric constant, and the imaginary part κ'' measures energy dissipation in the system, including that due to viscous damping of the rotational motion of the molecules in the alternating field. Measurements of κ' were used to locate the phase transition in the confined phase, since it exhibits large and sharp changes on freezing. Measurements of κ'' yield the dielectric relaxation time, τ . This characteristic time is very sensitive to the nature and structure of the phase. For example, $\tau \sim 10^{-9}$ s for liquids, 10^{-3} s for crystalline phases. Intermediate between these two phases are glassy phases ($\tau \sim 10^{-7}$ s) and hexatic phases ($\tau \sim 10^{-5}$ s). Thus the dielectric relaxation time is a sensitive measure of the nature of the phase, changing by orders of magnitude and giving important information about the nature of the phases observed. Evidence for the character of the phase transitions observed has been obtained using NDE measurements [10].

The NDE is defined as a change in the electric susceptibility induced by a strong electric field E :

$$\Delta\kappa' / E^2 = \kappa'^E - \kappa'^0 / E^2 \quad (2)$$

where κ'^E and κ'^0 are the electric susceptibility under an additional strong electric field E , and in its absence, respectively. The sign and magnitude of NDE of a liquid depends on the kind of inter- and intramolecular interactions and their energies [15]. The NDE vs. T divergence is typical of continuous phase transitions and its finite value is characteristic of NDE in confined systems [23,24]. The temperature dependence of the NDE near a phase transition temperature is described by a scaling law, and the value of the associated critical exponent can give information about the character of the phase transition that is observed.

For characterization of the nature of the liquid-walls interaction and also estimation of the pore size of ACF, we applied the electron paramagnetic resonance (EPR) method. EPR is a phenomenon in which particles with a non-zero magnetic moment (paramagnetic centres, i.e. unpaired electrons) are subjected to a constant and high-frequency alternate magnetic field adjusted to cause resonance absorption of energy. The transitions between the neighbouring energy levels of a particle [in a given energy state and in a given surroundings] are the sources of EPR signals. The resonance condition is:

$$h\nu = g\beta H \quad (3)$$

where ν is the frequency of the alternating field, (most often microwave), g is the spectroscopic splitting factor, β the Bohr magneton, and H is the intensity of the external magnetic field used to tune the system to resonance conditions. The surroundings of a paramagnetic centre can be the source of an additional local field, which permits characterisation of the energy state of the particle and its environment. We determine the spectroscopic splitting factor g (for a free electron equal to 2.0023). For a given substance it takes different values, and is a proportionality factor between the spin energy state and the magnetic field value. It can be treated as a parameter characterising the close environment of the particle studied. Additional information on the interaction of the paramagnetic centres and their interactions with the environment can be inferred from the fine or hyperfine structure of the spectrum.

The nano-porous materials that have been studied include controlled pore glasses (CPG) and Vycor, MCM-41 (a templated mesoporous material), and activated carbon fibers (ACF). The first three materials are silica-based, with pores that are roughly cylindrical. Vycor has pores of about 4.5 nm diameter, while CPG can have pore widths ranging from 7.5 nm to hundreds of nanometers. MCM-41 can have pore widths ranging from about 1.5 to 10 nm. The activated carbon fibers used were pitch based and had pore widths from 1.0 to about 1.6 nm. In the ACF the pores were roughly slit-shaped. All of these materials are relatively regular in their pore structure, and the pores are uniform in size, with little spread in pore width about the mean value. Comparison of results from these various materials provides information on the effects of pore shape (slit versus cylinder), size and nature of the surface. The ACF's have strongly adsorbing surfaces due to the close packing of the carbon atoms on the surface, while the silica-based materials have much more weakly attracting surfaces.

3. Molecular Simulation Studies

The conventional thermodynamic integration methods used to study freezing in bulk liquids fail for phases confined within pores, due to the presence of contact layer and other phases that arise due to the walls. To overcome the failure of the integration method, Radhakrishnan and Gubbins [14] used a method based on calculation of the Landau free energy, $\Lambda(\Phi)$, as a function of an effective bond order parameter, Φ . The Landau free energy is given by [15]:

$$\Lambda[\Phi] = -kT \ln(P[\Phi]) + C \quad (4)$$

where C is a constant, k is Boltzmann's constant and $P[\Phi]$ is the probability density of observing the system with an order parameter value between Φ and $\Phi+d\Phi$. The probability distribution function $P[\Phi]$ is calculated in a Grand Canonical Monte Carlo (GCMC) simulation using a histogram with umbrella sampling [17]. In-plane pair spatial and orientational correlation functions help identify the nature of the phases that correspond to the minima in the Landau free energy. The grand free energy, Ω , is calculated from the Landau free energy by:

$$\exp(-\Omega/kT) = \int d\Phi \exp(-\Lambda[\Phi]/kT) \quad (5)$$

This approach is not affected by phase changes in the contact layer, and can be used for repulsive, weakly attractive and strongly attractive walls.

Further Landau free energy studies, together with application of the Law of Corresponding States, show that for small adsorbate molecules the freezing behavior is largely controlled by a parameter $\alpha = c\varepsilon_{fw}/\varepsilon_{ff}$, which measures the ratio of the strength of the fluid-wall attraction to the fluid-fluid attraction [3,11]. Here ε_{fw} and ε_{ff} are the intermolecular potential well-depths for the fluid-wall and fluid-fluid interactions, and c is a parameter that accounts for the density and arrangement of the wall atoms. This enables global freezing phase diagrams to be constructed, showing the reduced freezing temperature vs. α , with regions corresponding to the various phases present (fluid, hexatic, contact layer, crystal, etc.). Comparisons with experimental data show good agreement in general. For small α , typically $\alpha < 0.8$ to 1.0, T_f is lower in the pore than in the bulk material, while for $\alpha > 0.8$ to 1.0 T_f is higher in the pore than in the bulk phase. For larger pores, where the number of adsorbed layers is greater than 2, contact layers also occur [11].

In two-dimensional systems, according to the Kosterlitz-Thouless-Halperin-Nelson-Young (KTINY) theory [18,19], melting involves two separate transitions; the first is a transition from a 2-d crystal (with positional and orientational order) to a hexatic phase (long-range orientational order, but positional disorder); the second occurs at a higher temperature and is from the hexatic to the liquid phase (positional and orientational disorder). The hexatic phase has been observed experimentally in thin films of liquid

crystals, using electron diffraction [20-22]; the diffuse electron intensity pattern displays a six-fold symmetry for hexatic phases. Hexatic phases have been clearly observed in our simulation studies of LJ fluids in carbons having narrow slit pores [10,11,14]. In these systems the strong adsorbate-wall attraction gives rise to pronounced layering of the adsorbate molecules. Each of these layers comprises a quasi-two-dimensional system. The crystal-hexatic and hexatic-liquid transitions are located by the Landau free energy method, and the hexatic phase shows the diffuse six fold symmetry in the structure factor, and other features characteristic of this phase. Recent DSC measurements on CCl_4 and aniline in activated carbon fibers show transitions that appear to correspond to crystal-hexatic and hexatic-liquid transitions; moreover, the transition temperatures agree within 5°C with those predicted in the simulations

4. Results and Discussion

4.1 DSC, DRS and NDE

Experimental studies have been carried out for carbon tetrachloride using DSC and for nitrobenzene using DSC and DRS in CPG, Vycor, MCM-41 and ACF [2-8]. In addition, aniline [8,10], benzene [8], water and methanol [9] have been studied in ACF. The studies in CPG, Vycor and MCM-41, all of which have roughly cylindrical, silica-based, pores, all showed a decrease in the freezing temperature, as predicted in the simulations. For the larger pores, of widths 7nm and greater, the depression of the freezing temperature was inversely proportional to the pore width, as predicted by the Gibbs-Thomson equation. For smaller pores, however, significant nonlinearity was observed indicating the breakdown of the Gibbs-Thomson equation. In addition to the freezing transition, evidence of a contact layer phase was obtained from the DRS experiments in many cases. The simulations predict such a phase, in which the adsorbed layer next to the pore wall has a structure (fluid or solid) different from that of the inner layers (solid or fluid). In these cases the experiments showed two relaxation times, one intermediate in magnitude between those of solids and liquids. For large cylindrical pores, $H > 20\sigma$, where σ is the diameter of the adsorbed fluid molecules, the adsorbate appeared to freeze to a crystalline structure, but for somewhat smaller pores only partial freezing occurred yielding a frustrated microcrystal structure together with amorphous regions. For pore diameters below 15σ only amorphous structures were observed.

In the case of activated carbon fibers, which possess strongly attractive walls, we observed a substantial increase (by as much as 60K) in the freezing temperature for both benzene and carbon tetrachloride. Such an increase had been previously observed by Kaneko et al. [12], and had been predicted in the simulations [8,10-13]. In the ACF the adsorbate phase is strongly layered, due to the small pore width (about 1.0-1.5 nm) and strong attractive forces from the carbon walls. We observe evidence of a stable hexatic phase that occurs between the crystal and liquid phases in these adsorbed layers. Such a hexatic phase had been predicted in the simulations for carbons with slit-shaped pores [10,11,14].

Recent NDE measurements on CCl_4 and aniline in activated carbon fibers show transitions that appear to correspond to crystal-hexatic and hexatic-liquid transitions; moreover, the transition temperatures agree within 5°C with those predicted in the

simulations. The pretransitional NDE anomalies have been described in terms of the phenomenological model of Landau – de Gennes [25,], used for the description of transitions from the liquid crystal phase to the isotropic phase, in which the presence of small liquid crystal regions of size $\xi(T)$ and uncorrelated orientations is assumed, and the size of the ordered regions are small when compared to the light wavelength. Then the intensity of the scattered radiation is $I \sim \xi^2$. Assuming the correlation range is in agreement with the scaling theory of KTHNY, the temperature dependence of NDE in the vicinity of the phase transitions in a quasi-two-dimensional system can be described as:

$$E^2/\Delta\kappa \sim \exp(-A / (T - T_c)^\gamma) \quad (6)$$

where $\gamma = 0.50$ for the transition liquid-hexatic phase, $\gamma = 0.37$ for the transition hexatic phase-crystal, and A is the amplitude. Fig. 1 presents the temperature dependence of NDE recorded for CCl_4 confined in ACF, in the vicinity of the two phase transitions noted. The solid lines in Fig. 1 correspond to the relation (9) for the appropriate values of the exponent γ . This result provides experimental verification of the presence of a stable hexatic phase in quasi-two-dimensional systems of small molecules.

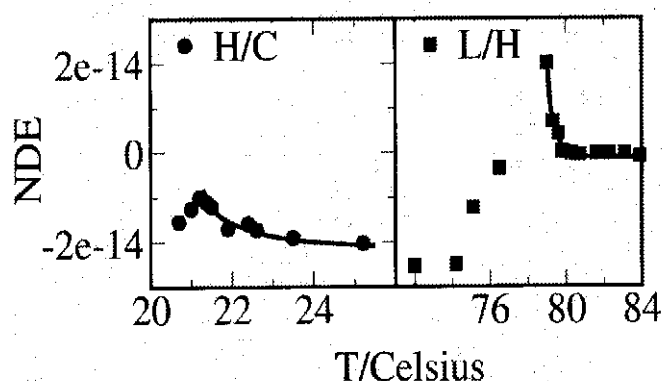


Figure 1. Temperature dependence of NDE for CCl_4 in ACF showing phase transitions: liquid to hexatic phase (L/H) and hexatic phase to crystal (H/C) [10].

4.2 EPR

In order to explain the nature of interactions of molecules with the pore walls we have undertaken a study by electron paramagnetic resonance. We wanted to determine whether the interactions are those typical of physical adsorption (van der Waals forces) and whether there are regions of specific interactions related to local irregularities of the pore walls or charge exchange in the interface for different pore materials. This paper presents results of the study on substances confined in graphite ACF pores.

EPR measurements of ACF (host) filled with various liquids: CCl_4 , C_6H_6 and $\text{C}_6\text{H}_5\text{NO}_2$ (guests), were performed in order to get information about the host \leftrightarrow guest interaction. When guest molecules are adsorbed in ACF voids a broader component of EPR signal appears for all studied systems. There is no EPR signal from guest molecules: no charge transfer from ACF to guest molecules – no hyperfine splitting arising from interaction with nuclear spins of H or N was observed. The strongest modification of the EPR spectrum of ACF was observed for ACF with $\text{C}_6\text{H}_5\text{NO}_2$. The EPR signal of ACF with $\text{C}_6\text{H}_5\text{NO}_2$ consists of three lines [26]. The narrow line – line width $\Delta B_{1s} \approx 0.3$ mT (line (1)) – is characteristic for pristine ACF. Its g-value is equal to g_{\perp} of graphite (= 2.0031) [27]. Its line width and g-factor are temperature-independent. Two broader components of the signal are also connected with the graphite structure of ACF. These are: line (2) with $\Delta B_{1s} \approx 1.7$ mT and $g = 2.0029$ (both temperature independent), and line (3) with strong ΔB_{1s} and g-factor temperature dependency: $\Delta B_{1s}(120\text{K}) \approx 13.2$ mT; $\Delta B_{1s}(4.2\text{K}) \approx 4.3$ mT; $g_{120\text{K}} = 2.0029$ and $g_{4.2\text{K}} = 1.9970$ (Fig.2). The line (2) originates from graphite particles (host) surrounded by guest molecules captured in nanopores. Similarly to component (1), the line width and g-factor are temperature independent. Broadening of the line (2), compared to (1), is caused by the shorter relaxation time of the more dense system. The line width and g-factor of the component (3) of the observed EPR spectrum strongly depends on temperature. Such behavior can be explained as a surface effect in ACF.

Stronger instabilities of paramagnetic centers at the surface of ACF or in its larger pores appear as a temperature effect. When temperature is lowered below 20 K, both line width and g-factor reach values characteristic for graphite nanoparticles surrounded by guest molecules captured in pores. No Dysonian shape of the EPR line is observed for each component. This shows that the ACF crystallite size is lower than $3.2 \mu\text{m}$ – the penetration depth of the microwave field in graphite. Each of the three lines obeys the Curie law. No hyperfine splitting from interaction with H or N nuclei, together with the Curie law for all three components, confirm the localization of paramagnetic centers within crystallites of ACF. According to the model of ACF proposed in [28] and the theory of EPR of small particles [29] these two effects make it possible to treat ACF as

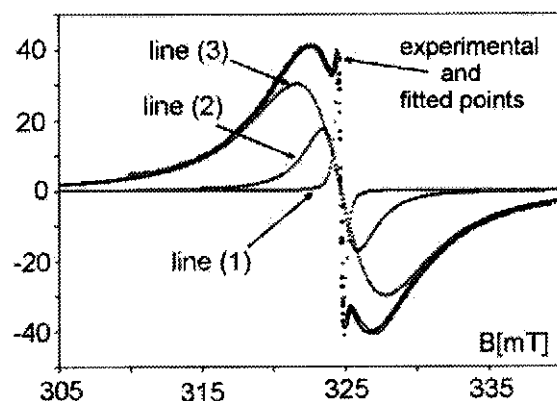


Figure 2. EPR spectrum for ACF filled with nitrobenzene; fit is a sum of lines (1),(2) and (3)

a system of nanographite particles in which quantum size effects can appear. Estimation based on the theory of EPR of small particles gives an average ACF nanocrystallite radius of 1.34 nm [26]. This value is in good agreement with the model of ACF proposed in [30] where graphite plates 1 – 3 layers thick and 2.5 nm in diameter are separated with nanopores of size 1-2 nm. The EPR results enable us to conclude that only weak host \leftrightarrow guest interactions occur in these systems; these lead to a modified EPR spectrum of pristine ACF, where van der Waals forces are significant.

5. Conclusions

As follows from the results of a dielectric study of the melting/ freezing phenomena of liquids confined in nanopores of different size and wall structure, and from the theoretical calculations, the qualitative behavior of these phenomena depends on a competition between the fluid-wall and fluid-fluid interactions, described by α parameter. When α is large, melting temperature increases on confinement. It has also been shown that even for simple fluids, several new phases appear: a few kinds of contact layer phases and hexatic phases. In cylindrical pores confinement effects are greater, but for pore diameters below $20\sigma_{\text{ff}}$ we do not observe crystallization, but either partial crystallization or glassy phases.

Taking into regard the significance of the type of interactions between the pore walls and the substance inside them, the strength of the interactions has been estimated for a few substances confined in the ACF pores by the EPR method. Results of this study have indicated the occurrence of van der Waals forces and the absence of strong local charge-transfer interactions between ACF pores and the substances within them.

6. Acknowledgments.

We are grateful for support of this research from the Polish Committee for Scientific Research (grant no.2 P03B 01424), the AMU Rector (grant no.2003) and the National Science Foundation (grant no. CTS-0211792). The international research cooperation was supported by a grant from NATO (grant no. PST.CLG.978802).

7. References

1. Eyraud, C., Quinson, J.F., and Brun, M. (1988), in K. Unger, J. Rouquerol, K.S.W. Sing, and H.Kral (eds.), *Characterization of Porous Solids*, Elsevier, Amsterdam, pp. 307-315.
2. Śliwińska-Bartkowiak, M., Gras, J., Sikorski, R., Radhakrishnan, R., Gelb, L.D., and Gubbins, K.E. (1999) Phase Transitions in Pores: Experimental and Simulation Studies of Melting and Freezing, *Langmuir* **15**, 6060-6069.
3. Radhakrishnan, R., Gubbins, K.E. and Śliwińska-Bartkowiak, M. (2000) Effect of the Fluid-Wall Interaction on Freezing of Confined Fluids: Towards the Development of a Global Phase Diagram, *Journal of Chemical Physics* **112**, 11048-11057.
4. Śliwińska-Bartkowiak, M., Dudziak, G., Sikorski, R., Gras, R., Radhakrishnan, R. and Gubbins, K.E. (2001) Melting/Freezing Behavior of a Fluid Confined in Porous Glasses and MCM-41: Dielectric Spectroscopy and Molecular Simulation, *Journal of Chemical Physics* **114**, 950-962.
5. Śliwińska-Bartkowiak, M., Gras, J., Sikorski, R., Dudziak, G., Radhakrishnan, R. and Gubbins, K.E. (2000) Experimental and Simulation Studies of Melting and Freezing in Porous Glasses, Unger, in K.K., Kreyss, G. and Baselt, J.P. (eds.), *Characterization of Porous Solids V*, Elsevier, Amsterdam, pp. 141-150.
6. Radhakrishnan, R., Gubbins, K.E., Śliwińska-Bartkowiak, M. and Kaneko, K. (2000) Understanding Freezing Behavior in Pores, in Do, D.D. (ed.), *Adsorption Science and Technology*, World Scientific, Singapore, pp. 234-238.
7. M. Sliwiska-Bartkowiak, G. Dudziak, R. Gras, R. Sikorski, R. Radhakrishnan, and K.E. Gubbins, "Freezing Behavior in Porous Glasses and MCM-41", *Colloids & Surfaces A*, **187-188**, 523-529 (2001).
8. Śliwińska-Bartkowiak, M., Dudziak, G., Sikorski, R., Gras, R., Gubbins, K.E., Radhakrishnan, R. and Kaneko, K. (2001) Freezing Behavior in Porous Materials: Theory and Experiment, *Polish Journal of Physical Chemistry*, **75**, 547-555 (2001).
9. Śliwińska-Bartkowiak, M., Dudziak, G., Sikorski, R., Gras, R., Gubbins, K.E. and Radhakrishnan, R. (2001) Dielectric Studies of Freezing Behavior in Porous Materials: Water and Methanol in Activated Carbon Fibers (2001) *Phys. Chem. Chem. Phys.* **3**, 1179-1184.
10. Radhakrishnan, R., Gubbins, K. E. and Śliwińska-Bartkowiak, M. (2002) Existence of Hexatic Phase in Porous Media, *Physical Review Letters* **89**, 076101-1-4.
11. Radhakrishnan, R., Gubbins, K.E. and Śliwińska-Bartkowiak, M. (2001) Global Phase Diagrams for Freezing in Porous Media, *Journal of Chemical Physics*, **116**, 1147-1155 (2002).
12. Kaneko, K., Watanabe, A., Iiyama, T., Radhakrishnan, R. and Gubbins, K.E. (1999) A Remarkable Elevation of Freezing Temperature of CCl₄ in Graphitic Micropores, *Journal of Physical Chemistry B* **103**, 7061-7063.
13. Radhakrishnan, R., Gubbins, K.E., Watanabe, A. and Kaneko, K. (1999) Freezing of Simple Fluids in Microporous Activated Carbon Fibers: Comparison of Simulation and Experiment, *Journal of Chemical Physics* **111**, 9058-9067.
14. Radhakrishnan, R. and Gubbins, K.E. (1999) Free Energy Studies of Freezing in Slit Pores: An Order-Parameter Approach using Monte Carlo Simulation, *Molecular Physics* **96**, 1249-1267.
15. Chelkowski A. (1993) *Physics of Dielectric*, 3rd edition, PWN, Warsaw
16. Landau, L.D. and Lifshitz, E.M. (1980) *Statistical Physics* 3rd edition, Pergamon Press, London.
17. Torric, G.M. and Valleau, J.P. (1974) Monte Carlo Free Energy Estimates Using Non-Boltzmann Sample: Application to the Sub-Critical Lennard-Jones Fluid, *Chemical Physics Letters* **28**, 578-585.
18. Kosterlitz, J.M. and Thouless, D.J. (1972), *Journal of Physics C* **5**, L124, *ibid.* **6**, 1181 (1973).
19. Halperin, B.I. and Nelson, D.R. (1978) Theory of Two - Dimensional Melting, *Physical Review Letters* **41**, 121-131; Nelson, D.R. and Halperin, B.I. (1979) Dislocation-Mediated Melting in Two Dimensions, *Physical Review B* **19**, 2457-2484; Young, A.P. (1979) Melting and the Vector Coulomb Gas in Two Dimensions, *Physical Review B* **19**, 1855-1866.
20. Brock, J.D., Birgenau, R.J., Lister, J.D. and Aharony, A. (1989) Liquids and Crystals and Liquid Crystal, *Physics Today* Volume, 52-59.
21. Chao, C.Y., Chou, C.F., Ho, J.T., Hui, S.W., Jin, A. and Huang, C.C. (1996) Nature of Layer-by-Layer Freezing in Free-Standing 40.8 Films, *Physical Review Letters* **77**, 2750-2757.

22. Chou, C.F., Jin, A.J., Huang, S.W. and Ho, J.T. (1998) Multiple-Step Melting in Two Dimensional Hexatic Liquid-Crystal Film, *Science* **280**, 1424-1426.
23. Gelb, L.D., Gubbins, K.E., Radhakrishnan, R. and Śliwińska-Bartkowiak, M. (1999) Phase Separation in Confined Systems, *Reports on Progress in Physics* **62**, 1573-1659.
24. Śliwińska-Bartkowiak M., Sowers S.I., Gubbins K.E. (1997) Liquid-Liquid Phase Equilibria on Porous Materials, *Langmuir* **13**, 1182-1188
25. deGennes P.G. (1974) *The Physics of Liquid Crystals*, Clarendon Press, Oxford
26. Kempański, M., Śliwińska-Bartkowiak, M. and Kempański, W., Host-guest interaction in ACF: EPR study, *this issue*
- Stankowski, J., Piekara-Sady, L., Kempański, W., Humiecki, O. and Szczaniecki, P. B. (1997) EPR of graphite and fullerenes, *Fullerenes Science and Technology* **5(6)**, 1203-1217
27. Fung, A.W. P., Wang, Z. H., Dresselhaus, M. S., Dresselhaus, G., Pełala, R. W. and Endo, M. (1994) Coulomb-gap magnetotransport in granular and porous carbon structures, *Physical Review* **B49**, 17325-17335
28. Buttet, J., Car, R. and Myles, Ch.W. (1982) Size dependence of the conduction-electron-spin-resonance g shift in a small sodium particle: Orthogonalized standing-wave calculations, *Physical Review* **B26**, 2414-2431.; Myles, Ch. W. (1982) Shape dependence of the conduction-electron spin-resonance g shift in a small sodium particle, *Physical Review* **B26**, 2648-2651.]